

An iterative model of diffuse illumination from bidirectional photometric data

Chung-Hao Tien,^{1,*} and Chien-Hsiang Hung²

¹ Department of Photonics and Display Institute, National Chiao Tung University, Hsinchu 30010, Taiwan

² Department of Photonics and Institute of Electro-optical Engineering, National Chiao Tung University, Hsinchu 30010, Taiwan

*chtien@mail.nctu.edu.tw

Abstract: This paper presents a methodology for including the photometric raw data sets into the diffuse illumination design process. The method is based on computing the luminance distribution on the outgoing side of diffusing elements from measured bidirectional scattering distribution functions (BSDFs). The model is limited to specimens that create rotationally symmetric scattering distribution. The calculation procedure includes the linear superposition and the correcting feedback. As an application example, the method is verified by a commercially available diffusing sheet illuminated by a 32-inch backlighting module. Close agreement (correlation coefficient = 98.6%) with the experimental measurement confirmed the validity of the proposed procedure.

©2009 Optical Society of America

OCIS codes: (120.5240) Photometry; (120.5820) Scattering measurements; (290.1483) BSDF, BRDF, and BTDF; (290.1990) Diffusion.

References and links

1. J. C. Stover, *Optical Scattering: Measurement and Analysis* (Mc Graw-Hill, New York, 1990).
2. M. Nieto-Vesperinas, *Scattering and Diffraction in Physical Optics* (Wiley, New York, 1991).
3. L. Tsang, J. A. Kong, and K. -H. Ding, *Scattering of Electromagnetic Waves, Theories and Applications* (Wiley, New York, 2000).
4. L. Tsang and J. A. Kong, *Scattering of Electromagnetic Waves, Advanced Topics* (Wiley, New York, 2001).
5. A. K. Fung, *Microwave Scattering and Emission Models and Their Applications* (Artech House, Boston, 1994).
6. A. Voronovich, "Small-slope approximation for electromagnetic wave scattering at a rough interface of two dielectric half-spaces," *Waves Random Media* **4**, 337-367 (1994).
7. A. Voronovich, *Wave Scattering from Rough Surfaces, 2nd Edition* (Springer-Verlag, Berlin Heidelberg, 1994).
8. K. E. Torrance and E. M. Sparrow, "Theory for off-specular reflection from roughened surface," *J. Opt. Soc. Am.* **57**, 1105-1114 (1967).
9. B. van Ginneken, M. Staveridi and J. J. Koendrik, "Diffuse and specular reflectance from rough surface," *Appl. Opt.* **37**, 130-139 (1998).
10. K. Tang and R. O. Buckius, "A statistical model of wave scattering from random rough surfaces," *Int. J. Heat Mass Transfer* **44**, 4095-4073 (2001).
11. L. Tsang, J. A. Kong, K. -H. Ding, and C. O. Ao, *Scattering of Electromagnetic Waves, Numerical Simulations* (Wiley, New York, 2000).
12. F. D. Hastings, J. B. Schneider, and S. L. Broschat, "A Monte Carlo FDTD technique for rough surface scattering," *IEEE Trans. Antennas Propag.* **43**, 1183-1191 (1995).
13. N. Garcia and E. Stoll, "Monte Carlo calculation for electromagnetic-wave scattering from random rough Surfaces," *Pgys. Rev. Lett.* **52**, 1798-1801 (1984).
14. K. Tang, R. Dimenna, and R. Buckius, "Regions of validity of the geometric optics approximation for angular scattering from very rough surface," *Int. Heat J. Mass Transfer* **40**, 49-59 (1997).
15. M. Bass, E. W. Van Stryland, D. R. Williams, and W. L. Wolfe, *Handbook of Optics, Volume II* (McGraw-Hill, New York, 1991).
16. E. Kreyszig, *Introductory Mathematical Statistics* (Wiley, New York, 1970).
17. J. de Boer, "Modelling indoor illumination by complex fenestration systems based on bidirectional : Basics, Measurement, and Rating," *J. Society for Information Display* **14/11**, 1003-1017 (2006).

18. M. E. Becker, "Evaluation and characterization of display reflectance," *Displays* **19**, 35-54 (1998).
 19. J. W. Goodman, *Introduction to Fourier Optics* (McGraw-Hill, New York, 2004)
 20. K. Iizuka, *Elements of Photonics I* (Wiley, New York, 2002)
 21. A. M. Nuijs and J. J. L. Horikx, "Diffraction and scattering at antiglare structures for display devices," *Appl. Opt.* **33**, 4058-4068 (1994).
 22. J. E. Harvey and C. L. Vernold, "Transfer function characterization of scattering surface," *Proc. SPIE* **3141**, 113-127 (1997).
 23. M. W. Hodapp, "Applications for High-Brightness Light-Emitting Diodes," in *Semiconductors and Semimetals Vol. 48*, G. B. Stringfellow and M. G. Craford ed., (Academic Press, San Diego, 1997) *Semiconductors and Semimetals Vol. 48*, Chap. 6, p. 227.
-

1. Introduction

Diffuse illuminations have been widely used for many fields, including projectors, liquid crystal displays, traffic signs, and luminaries. Generally, the diffusing components are the optical sheets that scatter a collimated incident light into a divergent angle in the transmittance space or the reflection space without spatial position shifts on the component surface. Here the light is diffused into a defined radiance angles for the purpose of beam shaping, brightness homogenizing, antiglare, directionality adjustment, and so on. Meanwhile, the rapid progress in the manufacture technologies also led to many new diffusing components for various purposes. To characterize the diffuse properties becomes essential for illumination design practice. However, a general and effective methodology for diffusing behavior in different area is still insufficient.

The diffuse phenomena are mainly caused by the optical scattering. Generally, scattering from the sheet components is caused by four mechanisms: surface topography, surface contamination, bulk index fluctuation and bulk particulates [1]. The physical phenomena involved in the scattering are most properly described by the Maxwell's equations with appropriate boundary conditions. The modeling approaches can be conducted by either analytical or numerical solution. The analytical approaches include Kirchhoff approximation [2-5], the small perturbation method [2,4], the integral equation method [5], the small slope approximation [6,7], the facet method [8-10], and so on. Besides, the numerical methods, such as finite-difference time-domain (FDTD) [11,12] and Monte Carlo ray-tracing [13,14], have also been developed. However, only one kind of mechanisms, such as surface topography, can be considered in one physics model, where a few conditions are assumed before the calculation. Unfortunately, the appearance of objects in the real world is usually modeled as a combination of these four mechanisms, which occur simultaneously and are mutually coupled. Thus, physically based models are still used only occasionally, both because of their complexity and that the parameters are not readily available. In addition, since the commercial diffusing components are quite discrepant from the individual supplier, to analyze the complex structures is not necessary. This paper presents a new calculation approach, which can directly calculate the output field of a diffusing sheet under arbitrary illumination.

In this study, we present the methodology, where the measured photometric raw data sets are imported into the iterative process. Firstly, we characterize the diffusing capability of tested sample in terms of bidirectional scatter distribution function (BSDF) [15]. Secondly, the sample will be illuminated by a reference Lambertian source which is decomposed into many elementary functions with respect to different weighting factors. Thirdly, the correlation coefficient [16] between the measured and simulation results would gauge the sampling number of BSDF superposition in the calculation process, and provide a feedback factor to ensure the modeling accuracy. Finally, the tested specimen will be illuminated by a commercially available 32-inch backlighting system to validate the methodology. The conclusions will show that the proposed approach can be used to accurately predict the diffused field in the laminating systems.

2. BS(T)DFs of Diffusing Components

Table 1. Nomenclature

	Abbreviations	Greek letters		Subscripts	
L	luminance (cd/m^2)	ω, Ω	solid angle (sr)	i	incident
E	illuminance (lx)	θ, ϕ	polar coordinates	t	transmitted
CC	correlation coefficient	τ	transmittance	c	calculated
W	weighting factor	Φ	light flux	e	experimental
q	bidirectional transmission distribution function (sr^{-1})	δ	delta function	j, m	count
				r	reference

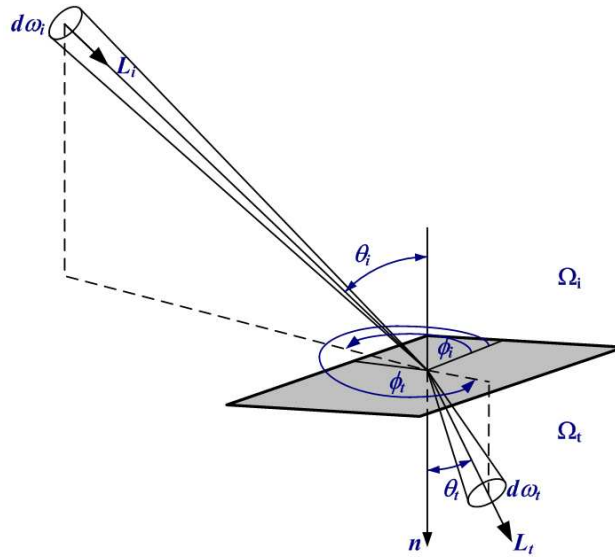


Fig. 1. Photometric and geometric quantities in the polar coordinate system.

2.1 Bidirectional Transmittance Distribution Function

In this section, we briefly review the characteristics and terminology of the bidirectional scatter distribution function (BSDF). The BSDF is typically split into reflected and transmitted components, which are treated separately as the bidirectional reflectance distribution function (BRDF) and the bidirectional transmittance distribution function (BTDF). The associated photometric and geometric quantities in polar coordinates are illustrated in Fig. 1, where all the scientific symbols and names through this paper are listed in Table 1. In order to simplify the analysis, we restrict the discussion to the transmissive type. Of course, the study can be easily applied to the reflective type without loss of generality. First of all, we define the bidirectional transmittance distribution function (BTDF) q [17] as following:

$$q(\theta_i, \phi_i, \theta_t, \phi_t) = \frac{dL_t(\theta_t, \phi_t)}{dE_i(\theta_i, \phi_i)} = \frac{dL_t(\theta_t, \phi_t)}{L_i(\theta_i, \phi_i) \cos \theta_i d\omega_i} \left[\frac{\text{cd}}{\text{m}^2 \text{lx}} \right], \quad (1)$$

where (θ_i, ϕ_i) and (θ_t, ϕ_t) represent the incident and transmitted angle of the light transmitting the specimen. BTDF describes the luminance dL_t , which is visible under the angles of

observation (θ_t, ϕ_t) , induced by the illuminance dE_i from an incident-side luminance L_i for an incident direction (θ_i, ϕ_i) with a solid angle $d\omega_i$. Since L_i is an available functional description, illuminance E can be decomposed into a linear combination of elementary functions. Equivalently, BTDF can be treated as the two-dimensional impulse response and completely describes the light spreading characteristics of a tested sample. The amount of light transmitted in the outgoing direction can be written as the integral of the BTDF multiplied by the incident flux from each incident direction (θ_i, ϕ_i) [17],

$$L_t(\theta_t, \phi_t) = \int_{\Omega} q(\theta_i, \phi_i, \theta_t, \phi_t) L_i(\theta_i, \phi_i) \cos \theta_i d\omega_i, \quad (2)$$

where L_t indicates the overall luminance distribution of the transmitted light. Also, the integral can be expressed in a discrete way as following:

$$L_t(\theta_t, \phi_t) = \sum_j q_j(\theta_{i,j}, \phi_{i,j}, \theta_t, \phi_t) L_{i,j}(\theta_{i,j}, \phi_{i,j}) \cos \theta_{i,j} \cdot \Delta\omega_j, \quad (3)$$

where $\Delta\omega_j$ indicates the solid angle around the specific incident angle $(\theta_{i,j}, \phi_{i,j})$. Based on the linear composition of every j -th components, the hemispherical luminance distributions over the transmission side can be solved accordingly.

2.2 BTDF measurement

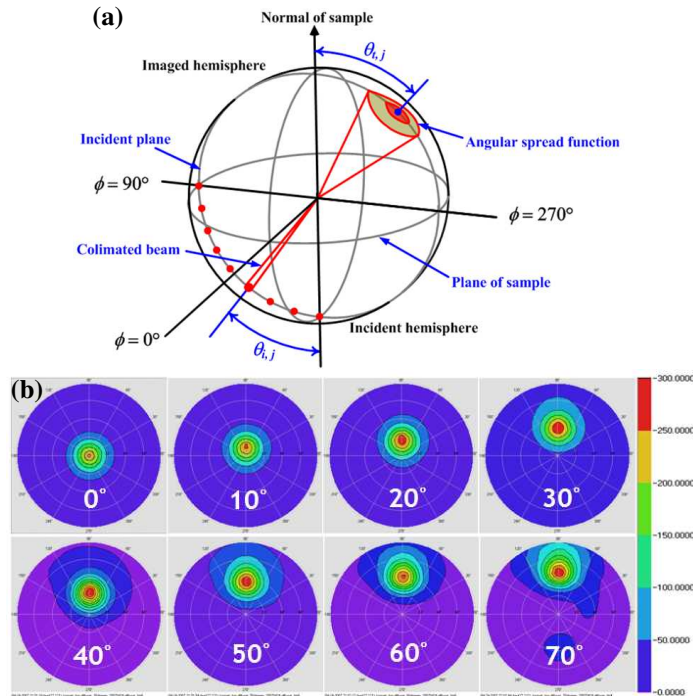


Fig. 2. (a) Schematic measurement setup of BTDFs, (b) the measured angular spread functions of an available diffuser.

BTDF measurement of a commercially available diffusing specimen for LCDs was performed by the conoscopic approach [17,18]. As the schematic description in Fig. 2(a), the specimen is illuminated by a collimated beams with a set of discrete incident directions $(\phi_i, \theta_{i,j})$, and the corresponding scattered light can be collected by an objective lens with moderate numerical aperture for observation of imaged hemisphere. Figure 2(b) shows a set of the measured angular spread functions of an arbitrary specimen with different incident polar angle θ_i along a

constant azimuthal angle $\phi_i = 90^\circ$. Every incident beam illuminating the specimen would lead to specific BTDFs. For the commercial diffusing sheets, the randomly distributed beads are in circular shape. Thus, the scattering fields, which are highly relevant to the geometric natures of the particulates, are circularly symmetric. As the measured BTDFs vary smoothly under different incident angle θ_i , the adequate angular sampling are sufficiently complete to represent the diffusing behavior. In this case, the angular interval $\Delta\theta_i$ was 10 degree.

2.3 Characterizations by BTDFs

BTDFs represent the angular spread function of the diffusing specimen, which have a variety of optical features due to various manufacturers' recipes about the refractive index, the size of scattering particles, the density of the bead distribution, and so on. In the following, we use the measured BTDFs to analyze two commercial diffusers with different bead sizes. As the tops of Fig. 3(a) and (b) show, the diffusive layer on the top of Polyethylene Terephthalate (PET) substrate has some beads buried in an acrylic binding layer and other beads protrude partially out of the binder layer. Here the beads are in a range of 10~25 μm . The bottoms of Fig 3 show the one-dimensional BTDFs. From the envelope of every transmitted peak, the diffusing power and particle size has a reciprocal relationship. For the case of a laser beam illuminating the diffusing structure with respectively different incident angles, the transmitted angular spectrum can be roughly found by the Fourier transform of the amplitude transmittance function of the bead aperture [19-21]. Thus, the smaller the bead size, the broader the scattering power after passing through the diffuser will be caused. This effect is entirely analogous to the broadening of the angular spectrum with the corresponding special frequency.

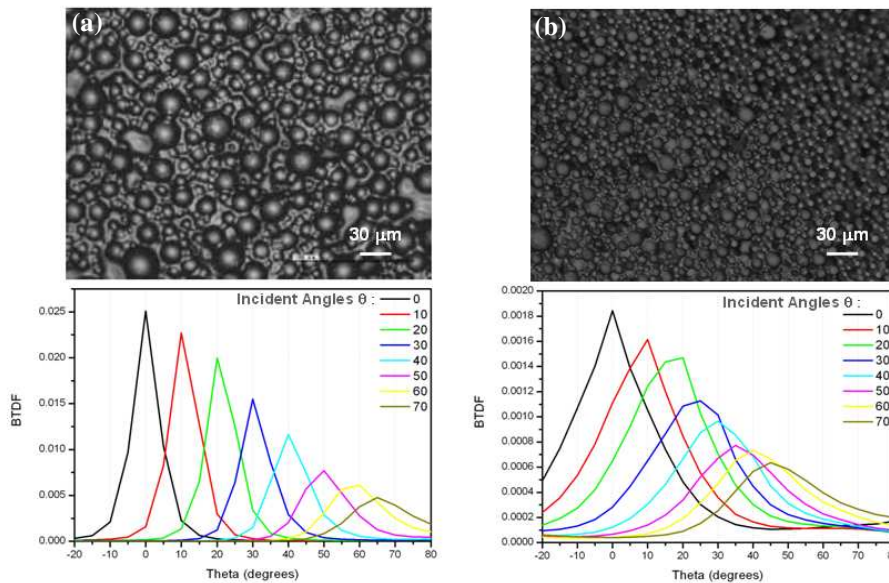


Fig. 3. The measured BTDFs and their corresponding OM pictures with (a) low spatial frequency and (b) high spatial frequency.

In addition to the dependence of scattering power on the particle size, there is another issue needed to be mentioned. As the definition, BTDF is simultaneously a function of the incident direction (θ_i, ϕ_i) and the transmitted direction (θ_t, ϕ_t) . J. E. Harvey [22] has mentioned that a general scattering surface has the shift-invariant behavior, which just requires one set of numerical data to completely characterize the scattering properties of a surface. The most conventional diffusers are circularly symmetric, so the variations of the incident impulse along azimuthal angle ϕ_i would be ignored. However, as shown in Fig. 3, the BTDFs exhibit a

discrepant scattering shape and peak shift with different inclining illumination. Especially, the phenomena are more observable in larger angles of incidence. Thus, in the incident side, BTDF is a function of pure inclination θ . A comprehensive model for such shift-variant system is essential for the diffuse illumination design flow.

3. Algorithm for modeling diffusers

The proposed procedure for modeling a diffusing specimen is shown in Fig. 4. The conception is to find the acceptable sampling points of the diffusing component through comparing the outgoing fields by our construction and the reference measurement. The algorithm is started with the aforementioned BTDF measurement. Based on the measured BTDFs, a rotational superposition was performed to implement the rotationally-constructed BTDFs (R-BTDFs). A rotationally symmetric source, that is practically available, illuminated on the sample for the purpose of calculation reference, and the luminance weights at different inclinations of the reference source were introduced into the R-BTDFs to calculate the outgoing field. After that, we will introduce a merit value (correlation coefficient) to compare the simulated far field luminance with the measured results. The correlation coefficient provides a feedback to correct the sampling point until the merit value converges to an acceptable value. In the following, the sample in Fig 3 (b) will be taken for the demonstration of the algorithm.

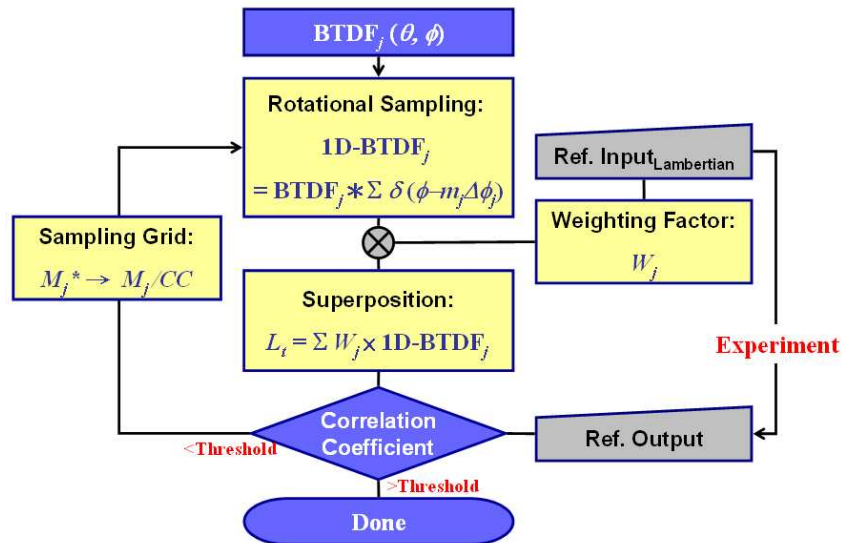


Fig. 4. Modeling procedure for a commercially available diffusing specimen.

3.1 Rotational Construction by BTDFs

Because the procedure is based on calculating the transmitted field by constructing the BTDFs, the rotational sampling of the BTDF is performed first. A rotationally symmetric field is assumed to illuminate the specimen. Therefore, the dependence along the azimuthal direction can be degenerated by taking convolution between the measured BTDFs q_j , which is the j -th inclination set as shown in Fig. 2, and a comb function along the azimuthal direction:

$$\begin{aligned}
 q_j^R(\theta_i, \phi_i) &= q_j(\theta_i, \phi_i) * \sum_{m_j=0}^{M_j} \delta(\theta_i - j\Delta\theta, \phi_i - m_j\Delta\phi_j) \\
 &= \sum_{m_j=0}^{M_j} q_j(\theta_i - j\Delta\theta, \phi_i - m_j\Delta\phi_j),
 \end{aligned}
 \tag{4}$$

where j and $\Delta\theta$ represent the shifts along θ direction with the interval $\Delta\theta$. m_j and $\Delta\phi_j$ indicate the shifts along ϕ direction of the j -th inclination. q_j^R is the j -th rotationally-constructed BTDF (R-BTDF). In our case, the width of the horizontal band $\Delta\theta$ is 10 degrees, which is mentioned in the measured results in section 2.2. Here the sampling number M_j , which means 2π is equally divided into M_j divisions, is increased with the outer band, so the sampling interval $\Delta\phi_j$ is varied with different j . Fig. 5 shows an numerical calculation of convolution of the 40°-inclination ($j=4$ the fourth ring) BTDF. Because of the nature of the integrated solid angle, the arrangement of M_j should be directly proportional to the zonal constant [23], which is a convenient factor to calculate the luminous flux emitted into a narrow band and multiplying the summation by a solid angle factor. After a number of straight manipulations, eight donut-like R-BTDF q_j^R can be obtained accordingly.

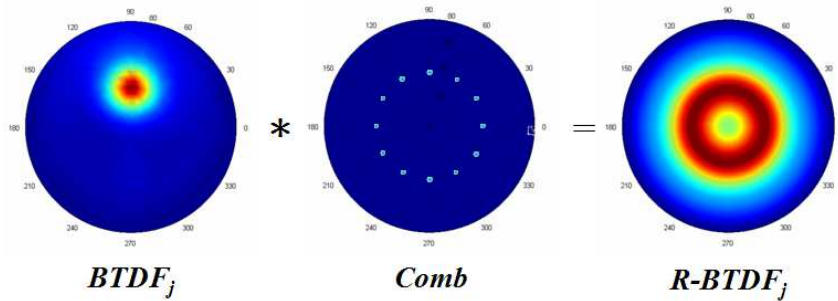


Fig. 5. The convolution of 40°-inclination ($j=4$) BTDF.

3.2. Weighting & Superposition of R-BTDFs

A rotationally symmetric reference light source is essential in the calibration of the algorithm. Usually, a Lambertian field is adopted due to its uniform luminance and easily offered by the conventional sources, which include the surfaces of fluorescent lamps or the light diffused by a thick diffusing plate. In our case, the measurement is performed by the setup where the light emitted from a tungsten lamp passes through a diffusion plate and Lambertian emission is measured by conoscopic system. In order to calculate the transmitted field under the reference illumination by BTDFs, each R-BTDF ($j=0\sim 7$) is weighted by the factor W_j in accordance with the Lambertian reference source subject to the corresponding inclinations. The weights W_j is the luminance at j -th inclination θ_j of the reference incident function $L_{i,r}$ over the value in normal direction θ_0 under a constant azimuth ϕ_0 .

$$W_{i,j} = \frac{L_{i,r}(\theta_j, \phi_0)}{L_{i,r}(\theta_0, \phi_0)} = \frac{L_{i,r}(\theta, \phi) \cdot \delta(\theta - j\Delta\theta, \phi - \phi_0)}{L_{i,r}(\theta, \phi) \cdot \delta(\theta - \theta_0, \phi - \phi_0)} \Bigg|_{\theta_0=0^\circ, \phi_0=90^\circ} \tag{5}$$

The scattering light field is determined by the superposition of the eight weighted R-BTDFs. Normalized luminance distribution of the transmitted light can be represented as:

$$\begin{aligned}
L_t(\theta_t, \phi_t) &= A \cdot \sum_{j=0}^J W_{i,j} \cos \theta_{i,j} \cdot q_j^R(\theta_t, \phi_t) \\
&= A \cdot \sum_{j=0}^J \sum_{m_j=0}^{M_j} W_{i,j} \cos \theta_{i,j} \cdot q_j(\theta_t - j\Delta\theta, \phi_t - m_j d_j),
\end{aligned} \tag{6}$$

where A is the normalized coefficient, and calculated by

$$A^{-1} = \sum_{j=0}^J \sum_{m_j=0}^{M_j} W_{i,j} \cos \theta_{i,j} \cdot q_j(\theta_t - j\Delta\theta, \phi_t - m_j d_j) \Big|_{\theta=0, \phi=0}.$$

Similar to Eq. (3), Eq. (6) has an identical form except the weighting factors W_j are introduced by the reference Lambertian source. Here the cosine term is a tilt factor between the light source and the illuminated plane. Fig. 6 exhibits the individual R-BTDFs and their superposition results, which means the constructed outgoing distribution. Although the normalized luminance distribution through the diffusing specimen from a Lambertian source is obtained, however, the accuracy of the calculation highly depends on the number of discrete sampling component. Consequently, an additional merit index is required to gauge the accuracy of the proposed algorithm. The amount of sampling number is sequentially increased and correlated with its measurement. In the absence of continuity, the algorithm would obtain the discrete points for BTDF superposition and keep the outgoing field in certain accuracy.

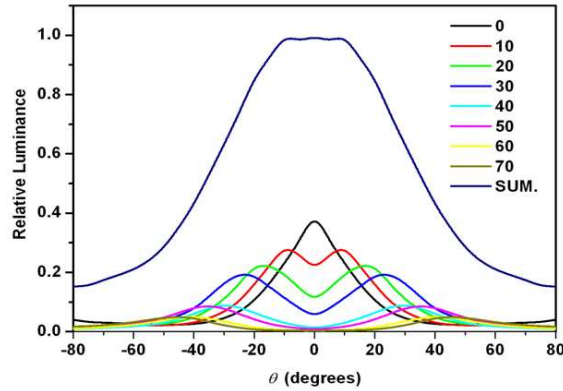


Fig. 6. The cross-section of individual 1D-BTDF and summation under Lambertian illumination.

3.3 Correlation Coefficient

Correlation coefficient is a merit value to gauge the accuracy of the numerical construction and served as a feedback for correcting the sampling points. Thus, we correlate the calculated field with its measurement, which are both the response of the reference Lambertian source. The correlation coefficient CC is defined as:

$$CC = \frac{\sum_{\theta} \sum_{\phi} [L_c(\theta, \phi) - \bar{L}_c][L_e(\theta, \phi) - \bar{L}_e]}{\sqrt{\sum_{\theta} \sum_{\phi} [L_c(\theta, \phi) - \bar{L}_c]^2 \sum_{\theta} \sum_{\phi} [L_e(\theta, \phi) - \bar{L}_e]^2}}, \tag{7}$$

where L_c and L_e are the normalized luminance distributions of the calculation and its measurement, respectively. \bar{L}_c and \bar{L}_e are the mean values of both corresponding datasets. If CC is below a threshold value T , it means the calculated field has a certain amount of discrepancy with the real one. Because the deviation is mainly due to the finite sampling points in the superposition, we would increase the sampling number ΣM_j by an incremental rate $\Sigma M_j \times CC^{-1}$ until CC is above the desirable threshold value. Eventually, the amount of the angular sampling ΣM_j along the azimuthal direction can converge to an acceptable value. In case of the commercially available diffuser in the Fig. 3(b), the correlation coefficient can be achieved upon 98% as the sampling number exceeds 357. Certainly, the sampling number is related to the optical complexity and dependent on the optical features by case. Because the retrieved output field is calculated by the superposition of finite number of BTDFs, the finite sampling points easily cause the discrete calculated fields or incorrect results. The profiles of BTDFs directly affect the required sampling number. The broader BTDF profile requires less sampling points, and the distribution is related to the structure of the diffusing sheets, as we mentioned in section 2.2.

4. Luminance Calculation

Aforementioned procedure is employed to determine the sampling grid of the BTDFs for calculating the optical response of the specimen, so we are able to directly apply the results to calculate the transmitted luminance distribution from assigned illuminating sources L_i . The weighting function $W(j, m)$ corresponding to the known sampling grid, can be obtained by:

$$W_{j, m_j} = \frac{L_i(\theta_j, \phi_{m_j})}{L_i(\theta_0, \phi_0)} = \frac{L_i(\theta, \phi) \cdot \delta(\theta - j\Delta\theta, \phi - m_j\Delta\phi_j)}{L_i(\theta, \phi) \cdot \delta(\theta - \theta_0, \phi - \phi_0)} \Bigg|_{\theta_0=0^\circ, \phi_0=90^\circ} \quad (8)$$

Thus, the transmitted distribution function can be calculated by two-dimensional superposition of the BTDFs multiplied by the corresponding weight function,

$$L_t(\theta_t, \phi_t) = \sum_j \sum_{m_j} W_{j, m_j} \cdot \cos \theta_{i, j} \cdot q_j(\theta_t - j\Delta\theta, \phi_t - m_j\Delta\phi_j). \quad (9)$$

In addition to the normalized luminance distribution, the absolute value is able to be calibrated by the transmittance $\tau(\theta)$ as following:

$$\tau(\theta_t) = \frac{\Phi_t}{\Phi_i(\theta_t)} = \int_{\Omega_i} \frac{L_t(\omega_t)}{E_i(\omega_t)} \cos \theta_t d\omega_t = \int_{\Omega_i} q(\omega_t, \omega_t) \cos \theta_t d\omega_t, \quad (10)$$

where the Φ_i and Φ_t are the overall luminous flux from the incident and transmitted sides of the diffusing sheet. In most case of diffusing sheets, the transmittances $\tau(\theta_t)$ are a constant with respect to different incident angles, so the absolute value of the transmittance can be applied on light sources with variant angular distributions. The transmittances τ can correct the normalized luminance distribution to absolute luminance value. The calculated result for the sample we mentioned is shown in Fig 7(a), where the transmitted luminance distribution was from a commercially available 32"-TV backlighting source. Comparing with the experimental results in Fig 7(b), the close agreement with the measurement ($CC = 98.6\%$) demonstrates the validity of the proposed training process and corresponding diffusing model. The negligible deviations at large angles were mainly resulted from the measurement errors attributed by the conoscope distortion.

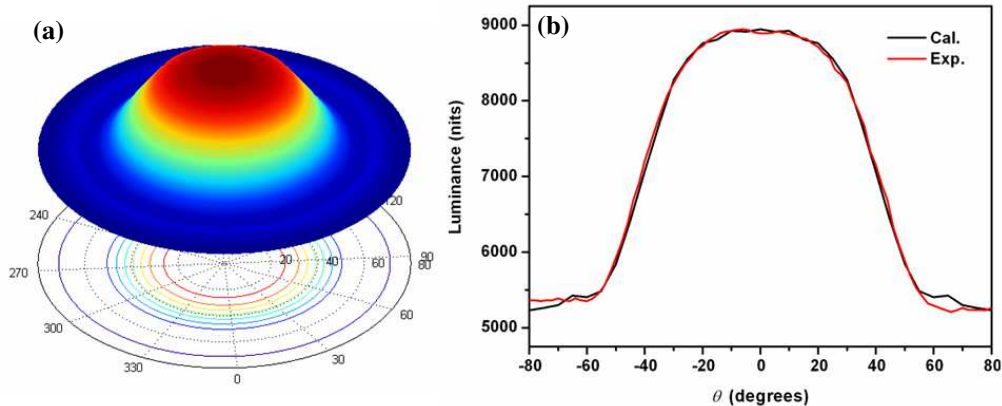


Fig. 7 Angular luminance distribution transmitted through the diffuser from a 32-inch backlighting source by (a) calculation, and (b) comparison of the cross-sections at $\phi = 0$ and 360 degree, where the CC between two curves is 98.6%.

5. Conclusions

A simple and effective algorithm to model the scattering characteristics of the diffuser is proposed and demonstrated. The major advantage of this study lies in that there is no need to formulate the complex physical mechanism of the scattering in a microscopic viewpoint. In stead, as long as a backlighting source (Cold Cathode Fluorescent Lamp or Light Emitting Diode) is available, proposed semi-quantitative algorithm can predict the optical radiance and efficiency with high precision without expense of computational time. The proposed algorithm is based on eight measured BSDFs and a reference Lambertian light source. Additional correlation coefficient is employed to evaluate the model accuracy and eventually converge to a stable sampling parameter. Thus, this modeling scheme only needs the BTDFs and the sampling parameter ΣM_j to characterize one diffusing sheet and it is convenient for designers or factories to build a diffuser database. We successfully demonstrate the validity by using a general backlight source, where calculated emergent luminance distribution is 98.6% close to the measurement. In most case, CC can achieve the value larger than 98%. The algorithm provides a relatively effective way for diffusing simulation, and is useful for the lighting development in display or luminance application.

Acknowledgment

The financial support from National Science Council, Taiwan, under contract NSC 96-2221-E-009-114-MY3 and Kismart Corporation is acknowledged.